

Serum amyloid A mediates the inhibitory effect of *Ganoderma lucidum* polysaccharides on tumor cell adhesion to endothelial cells

YING-BO LI¹, RUI WANG¹, HONG-LI WU¹, YU-HUA LI¹, LI-JUN ZHONG², HE-MING YU³ and XUE-JUN LI¹

¹Department of Pharmacology, School of Basic Medical Sciences and State Key Laboratory of Natural and Biomimetic Drugs; ²Medical and Health Analytical Center, Peking University, Beijing 100083;

³National Research Institute for Family Planning, Beijing 100081, China

Received March 18, 2008; Accepted May 9, 2008

DOI: 10.3892/or_00000041

Abstract. *Ganoderma lucidum* polysaccharides (GIPS) are the major bioactive composition of *Ganoderma lucidum*, a well-recognized oriental medical fungus. The published data have shown a complementary effect of GIPS in cancer therapy. The present study was designed to determine the anti-tumor efficacy of GIPS and the possible mechanism covering this effect. Murine Sarcoma 180 (S180) model was established, and GIPS administered orally for 10 days. On the 10th day, tumors were weighed to assess the inhibitory effect of GIPS and sera were collected for proteomic analysis and *in vitro* study. The *in vivo* results demonstrated that 25, 50 and 100 mg/kg GIPS inhibited S180 growth by 32.67, 44.80 and 45.24%, respectively ($P < 0.01$). Proteomic study revealed marked protein changes after the process of treatment. Three significantly changed proteins were identified by ESI-Q-TOF-MS and database search indicated that they were haptoglobin, apolipoprotein A-II and serum amyloid A (SAA), respectively. Additionally, the expression change of SAA was confirmed by both Western blot and RT-PCR. The adhesion assay showed that GIPS-treated sera dramatically inhibited the adhesion ability of human prostate carcinoma (PC-3M) cells to human umbilical cord vascular endothelial cells (HUVECs), and this effect partially recovered after immunodepletion by the antibody against SAA. Collectively, these results suggest that GIPS inhibited the tumor growth and tumor cell adhesion to HUVECs via up-regulation of SAA protein expression.

Introduction

Ganoderma lucidum (Leyss. ex Fr.) Karst, also known as 'Lingzhi' in China, has a long history of medical use in Asian countries. This medical mushroom, which was used to promote health and longevity in the past, has been recently shown to have therapeutic effects on many diseases, including neurasthenia, insomnia, nephritis, hepatitides, diabetes and cardiovascular disease (1-5). Especially, it shows prominent anti-tumor actions. In the 70s, T. Sasaki uncovered the anti-tumor effect of polysaccharides from *Ganoderma applanatum* (another species of *Ganoderma*) for the first time (6). From then on, both *in vivo* and *in vitro* research on the anti-tumor activity of *Ganoderma lucidum* have been carried out, supporting its application for cancer treatment and prevention. In addition, *Ganoderma lucidum* exhibited adjuvant role in combination with radiotherapy or chemotherapy. It can enhance the anti-tumor effect of chemotherapeutics. According to these reports, the main anti-tumor components in *Ganoderma lucidum* are polysaccharides (7) and triterpenoids (4), which are the main biological compounds of water extracts and alcohol extracts.

Because one of the effective ways to develop new drugs from bioactive compounds of natural products is to find the potential protein targets, the study on the molecular mechanisms of anti-tumor effect of GIPS has received much attention. Previous studies proposed that the cancer prevention activity of GIPS were carried out mainly through immunomodulation (7). However, some recent studies suggested other potential mechanisms, such as anti-angiogenesis (8), inhibition of tumor cell motility (9), induction of apoptosis (10), induction of phase II-metabolizing enzyme (11) and antimutagenic activities (12). Nevertheless, the mechanisms of anti-tumor activities of GIPS remain obscure. In order to better understand the anti-tumor mechanisms of GIPS, two-dimensional gel electrophoresis analysis was adopted in this study. Through analyzing global protein profile in GIPS-treated and control S180 mice coupling with mass spectrometry, we attempted to elucidate the possible anti-tumor mechanisms and find potential protein targets of GIPS. We observed the possible functions of one dramatically changed protein by cell-based research and compared the effects of

Correspondence to: Dr Xue-Jun Li, Department of Pharmacology, School of Basic Medical Sciences and State Key Laboratory of Natural and Biomimetic Drugs, Peking University, Beijing 100083, China

E-mail: xjli@bjmu.edu.cn

Key words: *Ganoderma lucidum* (Leyss. ex Fr.) Karst, polysaccharides, anti-tumor, two dimensional gel electrophoresis, mass spectrometry, serum amyloid A, adhesion

GIPS-treated sera on the tumor cell adhesion ability to HUVECs with and without depleting of this protein. These findings provide preliminary evidence for a novel mechanism by which *GIPS* exerts its anti-tumor effect.

Materials and methods

Animals and drugs. Inbred male BALB/c mice weighing 17–22 g were purchased from the Department of Experimental Animals, Peking University Health Science Center, Beijing, China. All procedures were in accordance to the Institute Ethics Committee for Experimental Use of Animal. *Ganoderma lucidum* polysaccharides (*GIPS*) are gift from Professor Zhi-Bin Lin, Department of Pharmacology, Peking University Health Science Center. *Ganoderma lucidum* (Leyss. ex Fr.) Karst was collected in Fujian Province, China. The fruit body of *Ganoderma lucidum* (Leyss. ex Fr.) Karst was authenticated by Professor Xiao-Lan Mao, Institute of Microbiology of Chinese Academy of Science. *GIPS* was extracted by hot water from the fruiting body of *Ganoderma lucidum* (Leyss. ex Fr.) Karst, followed by ethanol precipitation, reserve dialysis and protein depletion. The yield of *GIPS* was 0.82% (w/w) in terms of the fruiting body of *Ganoderma lucidum*. It is a polysaccharide peptide with a molecular weight of 584900 and has 17 amino acids. The ratio of polysaccharides to peptides is 93.51:6.49%. The polysaccharides consist of rhamnose, xylose, fructose, galactose, mannose and glucose with molar ratios of 0.793:0.964:2.944:0.167:0.384:7.94 and are linked by h-glycosidic linkages. It is a hazel-colored and water-soluble powder (4).

Sample preparation. Murine Sarcoma 180 (S180) cells were purchased from Beijing Tumor Institute and maintained by weekly transplantation of the tumor cells into the peritoneal cavity of mice. S180 cells (2×10^6 /mouse) were injected into the axillary fossa of the right foreleg. On the second day after inoculation, mice were separated into 4 groups ($n=10$) to receive saline, or 25, 50, 100 mg/kg *GIPS* dissolved in saline orally once a day. On the 10th day after drug treatment, the mice were sacrificed and tumors were excised and weighed. At the same time, the serum samples and liver samples were separated and stored at -70°C until use.

Cell culture. Human umbilical cord vascular endothelial cells (HUVECs) were isolated by 1% collagenase (Invitrogen, USA) from human umbilical cords, and were cultured in M199 (Gibco, USA) supplemented with 20% heat-inactivated fetal bovine serum (FBS, Gibco), 40 $\mu\text{g/ml}$ endothelial cell growth supplement (ECGS, purchased from China-Japan Friend Hospital), 100 U/ml penicillin, 100 U/ml streptomycin, 50 $\mu\text{g/ml}$ heparin and 300 $\mu\text{g/ml}$ *L*-glutamine. HUVECs were identified by the typical polygonal morphology and by detecting their immunoreactivity of factor-VIII related antigens. Human prostate carcinoma cells (PC-3M) were cultured in RPMI-1640 (Gibco) supplemented with 10% fetal bovine serum, 100 U/ml penicillin and 100 $\mu\text{g/ml}$ streptomycin.

Two dimensional gel electrophoresis and image analysis. The protein concentration of serum samples was measured by Bradford method. Serum protein (1 mg) was dissolved in

the rehydration buffer (8 M urea, 4% CHAPS, 65 mM DTT, 0.2% Bio-Lyte, 0.001% bromochlorophenol blue) to a final volume of 300 μl . This mixture was then applied to two-dimensional electrophoresis. The first dimension isoelectric focusing (IEF) was performed using 18 cm, pH 3–10, linear immobilized pH gradients gel (IPG) strips (Amersham Pharmacia Biotech, USA). The IPG strips were rehydrated for 16 h at 20°C by placing the strips gel-side-down and covered with mineral oil. Then, IEF was performed at 20°C in following steps: 250 V linear for 0.5 h, 1000 V gradient for 1 h, 8000 V linear for 5 h, 8000 V gradient until 60000 Vh. After IEF, the IPG strips were equilibrated in buffer containing 6 M urea, 20% glycerol, 0.375 M Tris-HCl (pH 8.8), 2% SDS and 20 mg/ml DTT for 15 min, and then for another 15 min in the same buffer with 25 mg/ml iodoacetamide replacing DTT. Then, the second dimension was proceeded on 12% SDS-PAGE gels at 10 mA/gel for 30 min followed by 20 mA/gel until completion. Gels were stained with Coomassie blue or silver. The experimental procedures were repeated more than three times. Then, 2D gels were analyzed using the PDQuest software (Bio-Rad) according to the protocols provided by the manufacturer. All gel spots that detected as significantly changed were then highlighted and checked manually to prevent any artifacts due to gel distortions, inappropriately matched or mistakenly detected spots.

Protein identification by ESI-Q-TOF-MS/MS. The selected protein spots were excised from the gels for decolorization, in-gel digestion and MS analysis. Electrospray quadrupole/time-of-flight mass spectrometry (ES-Q-TOF-MS, Waters, USA) was performed to identify the selected protein spots. The peptide mixture was carried out on a Waters Capillary liquid chromatography system including three pumps A, B and C (Waters). Fused silica tubing (75 μm x 100 mm) packed with symmetry 300TM C₁₈, 3.5 μm spherical particles with pore diameter 100 Å (Waters) The flow rate was set at 2.5 $\mu\text{l/min}$. Samples were injected at a flow rate of 20 $\mu\text{l/min}$ with pump C and salts were removed on the precolumn of (0.35x5 mm) packed with symmetry 300TM C₁₈, 3.5 μm spherical particles with pore diameter 100 Å (Waters). The precolumn was connected in the 10-port switching valve, and switched to the analytical column after the sample was desalted. Mobile phase A consisted of water/ACN (95/5, v/v) with 0.1 FA. Mobile phase B consisted of water/ACN (5/95, v/v) with 0.1 FA. The separation was performed by running an online gradient: 3% B, for 0.1–3.5 min for injection; 5–40% B, for 3.5–40 min; 40–60% B, for 40–60 min; 60–90% B, for 60–65 min; 90–5% B, for 65–70 min; 5–5% B, for 70–90 min. The Cap LC is coupled on-line with a Q-TOF Ultima Global mass spectrometer (Waters) for detection and protein identification. Peptide mixtures were dissolved with 2 μl 0.1% FA and inject by the atmosphere on the precolumn using a Cap LC system. Peptides were directly eluted into a Q-TOF mass spectrometer (Q-TOF Ultima Global mass spectrometer; Waters) at 250 nl/min on the analytical column. After being processed with Mass Lynx 4.0, the data resulting from the MS/MS analysis were applied for identification with MASCOT search engine (<http://www.matrixscience.com>).

Western blot analysis. A sample consisting of 80 μ g of protein was separated by 15% polyacrylamide gels at 150 V constant power. Protein was then transferred electrophoretically at 200 mA to a polyvinylidene difluoride (PVDF) immobilion-P membrane (0.22 μ m pore size; Millipore Corp., USA) in a transfer buffer (pH 8.3) composed of 25 mM Tris-HCl, 192 mM glycine and 20% methanol at 4°C for 2 h. The membranes were blocked with Tris-buffered saline (TBS, 100 mM Tris-HCl and 0.9% NaCl, pH 7.5) containing 5% non-fat milk for 1 h at room temperature, and subsequently incubated with anti-SAA antibody (Biosource, USA) at a 1:1000 dilution at 4°C overnight. After three washes in TBS containing 0.1% Tween-20 (TBS-T), the membranes were incubated with 1:1000 HRP-conjugated secondary antibody with 5% non-fat milk for 1 h and visualized using the chemiluminescent ECL reagent.

Semi-quantitative RT-PCR analysis. For semi-quantitative reverse transcriptase-polymerase chain reaction (RT-PCR) analysis, total-RNAs were extracted from the liver samples of each group. The RNA concentration was determined by measuring the absorbance at 260 nm, and its quality monitored by 0.8% agarose gel electrophoresis. Reverse transcription was carried out at 37°C for 60 min, followed by 95°C for 2 min and first round PCR for 95°C for 30 sec, 55°C for 30 sec, 72°C for 30 sec and final extension at 72°C for 5 min. Primers used in this study were as follows. SAA (5'-GCCTGGTCTTCTGCTCCCTG-3' and 5'-CCACTGCGGCCATGTCTGTT-3') and β -actin (5'-ATCATGTTTGAGACCTTCAACA-3' and 5'-CATCTCTTGCTCGAAGTCCA-3'). mRNA levels of β -actin were used to normalized the amount of RNA.

Cell adhesion assay. PC-3M cells were cultured in RPMI-1640 supplemented with 100 mg/l CFDA (Sigma, USA) for 30 min at 37°C, then washed three times by PBS to remove the residue fluorescent dye. Cells viability was examined by trypan blue staining method and was not affected by this protocol.

HUVECs were cultured in 96-wells culture plate until confluence. Then the medium with control sera and *GLPS*-treated sera (25, 50, 100 mg/kg) were changed respectively and cultured for 48 h. And then the medium was removed, CFDA-labeled tumor cells (10^4 /well) were added to 96-wells culture plate, and cocultured with HUVECs for 30 min at 37°C. After cells were washed by PBS for three times, the number of adherent tumor cells was counted under fluorescent microscope in five fields each well (13).

Immunodepletion of SAA. Control sera and *GLPS*-treated sera were incubated with anti-human SAA monoclonal antibody (Biosource; 1:50 dilution) for 1 h at 4°C, and then incubated with protein A-Agrose (Sigma, USA) for 12 h on a roller system at 4°C. After centrifugalization at 15000 rpm for 10 min, the protein A-Agrose was removed. Then the immunodepleted sera were used for the adhesion assay.

Statistical analysis. Data were analyzed by one-way analysis of variance (ANOVA), followed by Dunnett's test (SPSS 10.0 software). Results are presented as means \pm SD. $P < 0.05$ was considered to be statistically significant.

Table I. The inhibitory effect of *GLPS* after oral treatment for 10 days on the growth of Sarcoma 180 in Balb/c mice.

Group	Dose (mg/kg)	Body weight (g)	Tumor weight (g)	Inhibitory rate (%)
Control	-	18.9 \pm 1.7	1.10 \pm 0.11	-
	25	19.4 \pm 1.5	0.76 \pm 0.14 ^a	32.67
<i>GLPS</i>	50	19.3 \pm 1.2	0.61 \pm 0.12 ^a	44.80
	100	18.2 \pm 1.4	0.58 \pm 0.16 ^a	45.24

Calculation of the inhibition rate based on the following formula: tumor inhibition rate (%) [(average tumor weight of control group - average tumor weight of *GLPS* group)/average tumor weight of control group] \times 100%. Values are mean \pm SD, n=6. ^a $P < 0.01$ vs control group. *GLPS*, *Ganoderma lucidum* polysaccharid.

Results

Inhibitory effect of *GLPS* on tumor growth. As shown in Table I, after the oral administration of 25, 50 and 100 mg/kg *GLPS* for 10 contiguous days, the growth of tumor was inhibited by *GLPS* in S180 mouse model, and the tumor inhibition rate was 32.67, 44.80 and 45.24%, respectively, which was identical with published studies by other groups.

2D gel electrophoresis and ES-Q-TOF-MS analysis on the sera of *GLPS*-treated and control mice bearing murine sarcoma 180 tumors. The serum samples from the control group and *GLPS*-treated groups were analyzed by 2D gel electrophoresis. Comparing the protein profiles by PDQuest software analysis, over 500 serum protein spots were recognized in each gel. Among them, three protein spots which were well separated (Fig. 1) were cut off from Coomassie blue-stained gels and subjected to ES-Q-TOF-MS analysis. Combining with database search, the spots were identified as haptoglobin, apolipoprotein A-II and serum amyloid A, respectively. The data are summarized in Table II. The MS/MS results of the three identified proteins are shown in Fig. 2.

Validation of differentially expressed protein by Western blot analysis. Through functional exploring of the three identified proteins, serum amyloid A (SAA) was chosen for further study. To confirm the identification and expression change of SAA, sera were analyzed by Western blot for validation. As shown in Fig. 2C, the serum level of SAA was increased in S180 mouse model after the treatment of *GLPS*, and this result was consistent with the 2D gel electrophoretic analysis.

Validation of differentially expressed protein by semi-quantitative RT-PCR analysis. In previous research, SAA protein in the serum was suggested to be of liver origin (14), therefore, the SAA levels in liver samples were examined by semi-quantitative RT-PCR analysis for further validation.

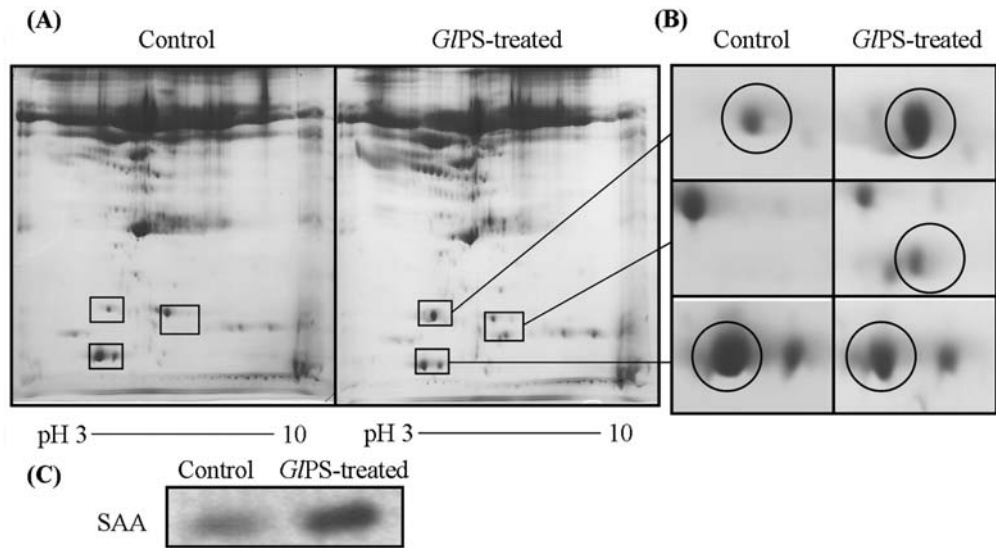


Figure 1. (A) Profiles of serum proteins from mice in control group and *GIPS*-treated group by 2D. The IEF was for pH 3-10. (B) The enlarged local images of proteins in the 2D gels. Proteins in serum from mice inoculated with Sarcoma 180 subjected to identification by MS are marked by circles. (C) Western blot analysis of SAA expression in serum of S180 mouse model with or without the treatment of *GIPS*. SAA level in serum increased after the treatment of *GIPS*. Control, serum sample from mice in control group; *GIPS*-treated, serum sample from mice in 100 mg/kg *GIPS*-treated group.

Table II. ES-Q-TOF-MS identified proteins in control serum vs *GIPS*-treated serum. The Swiss-Prot accession number, protein name, the % coverage of analyzed peptides, the score from Mascot searches and M_r are shown for each protein.

Spot no.	Accession no.	Protein name	% coverage	Score	PI	M_r (Da)
1	gi8850219	Haptoglobin [Mus musculus]	4	59	5.88	38727
2	gi7304897	Apolipoprotein A-II [Mus musculus]	25	212	4.9	11312
3	gi200904	Serum amyloid A	34	355	6.21	12876

The results are shown in Fig. 3. The mRNA level of SAA was up-regulated in a dose-dependent manner. The pattern of change was in agreement with 2D results, so the results of RT-PCR analysis confirmed the reliability of comparative proteomic study.

Inhibition effect of GIPS-treated sera on the adhesion ability of PC-3M to HUVECs. The effect of *GIPS*-treated sera on the metastatic adhesion function of malignant cells was evaluated by testing its effect on PC-3M cell adhesion to HUVECs monolayers. It is clear from Fig. 4 that 25, 50 and 100 mg/kg *GIPS*-treated sera can significantly inhibit the attachment of PC-3M cells to HUVECs, respectively ($P<0.01$). Meanwhile, examined by MTT method, no cytotoxic effect on HUVECs was seen at the same concentrations (data not show).

SAA-immunodepleted sera partially abolish the inhibition ability of GIPS-treated sera on the adhesion of PC-3M to HUVECs. After removal of SAA by immunodepletion with anti-SAA antibody in control and *GIPS*-treated sera, the cell adhesion assay was carried out using immunodepleted sera. As shown in Fig. 5. SAA-depleted *GIPS*-treated sera (25 and 50 mg/ml) showed no inhibition effect on adhesion ability of PC-3M cells to HUVECs comparing with the control group,

but 100 mg/ml SAA-depleted *GIPS*-treated serum still exerted significant inhibition ability. The inhibitory effect of *GIPS*-treated sera on adhesion ability of PC-3M to HUVECs was partially abolished after the depletion of SAA.

Discussion

The anti-tumor activity of *GIPS* has been widely studied both *in vitro* and *in vivo*. In agreement with these findings, our results listed in Table I revealed that *GIPS* inhibited the growth of Sarcoma 180 by 32.67, 44.80 and 45.24%, respectively.

Cancer is a multisteps and complex process that attributes to protein changes at functional level. The proteins change as the components or the ultimate effectors in the altered signaling pathways lead to cancer survival, growth, invasion and metastasis (15). Therefore, analyzing protein changes on tumor tissue or sera in animals bearing cancer will be helpful in uncovering the mechanisms of this pathological process and discovering anti-tumor drugs. As a high-throughput approach of mapping and analyzing protein profiles, proteomic methods show great advantages in cancer research. It offers scientists a feasible approach to explore global protein alterations rather than limited ones. The

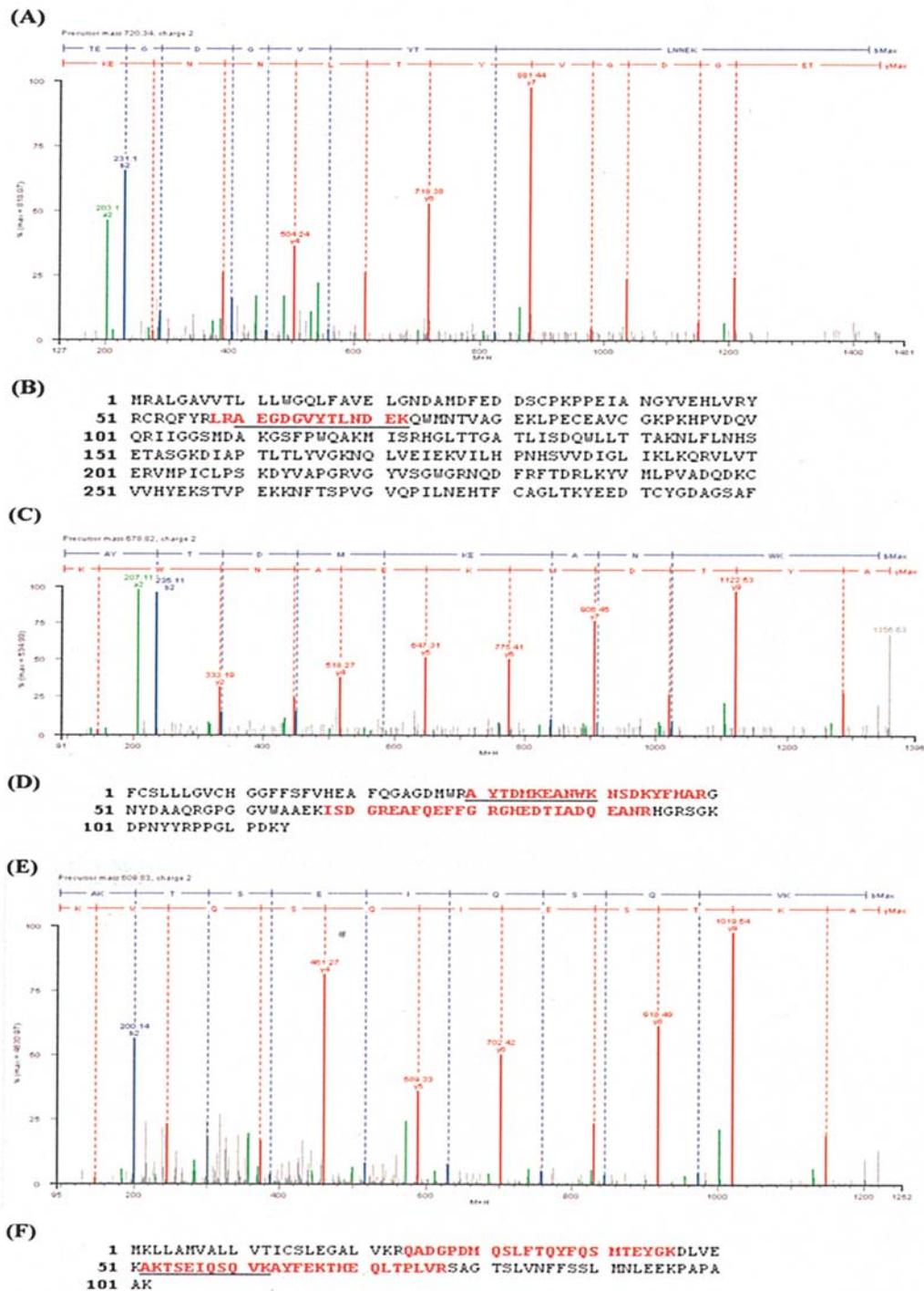


Figure 2. ESI-Q-TOF-MS analysis of differentially expressed proteins. (A) The amino acid sequence of a double charged peptide with m/z 720.34 was identified as TEGDGVYTLNNEK from mass differences in the y-fragment ions series, and matched with residues 60-72 of haptoglobin [Mus musculus]. (B) Protein sequence of haptoglobin precursor is shown. Matched MS/MS fragmentation is underlined. (C) The amino acid sequence of a double charged peptide with m/z 609.832 was identified as AKTSEIQSQVK from mass differences in the y-fragment ions series, and matched with residues 52-62 of apolipoprotein A-II [Mus musculus]. (D) Protein sequence of apolipoprotein A-II is shown. Matched MS/MS fragmentation is underlined. (E) The amino acid sequence of a double charged peptide with m/z 678.82 was identified as AYTDHKEANWK from mass differences in the y-fragment ions series, and matched with residues 30-40 of serum amyloid A. (F) Protein sequence of serum amyloid A is shown. Matched MS/MS fragmentation is underlined.

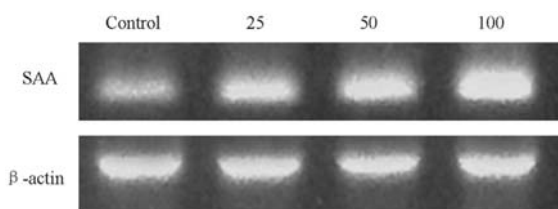


Figure 3. Semi-quantitative RT-PCR analysis of SAA mRNA expression in liver samples of S180 mouse model with or without the treatment of different dose of G/PS. Total-RNA was extracted and amplified by RT-PCR using gene-specific primers. Control, liver sample of mice in control group; 25, 50 and 100, liver samples of mice in G/PS-treated groups (25, 50 and 100 mg/kg, respectively); SAA RT-PCR product length, 304 bp; β-actin RT-PCR product length, 540 bp.

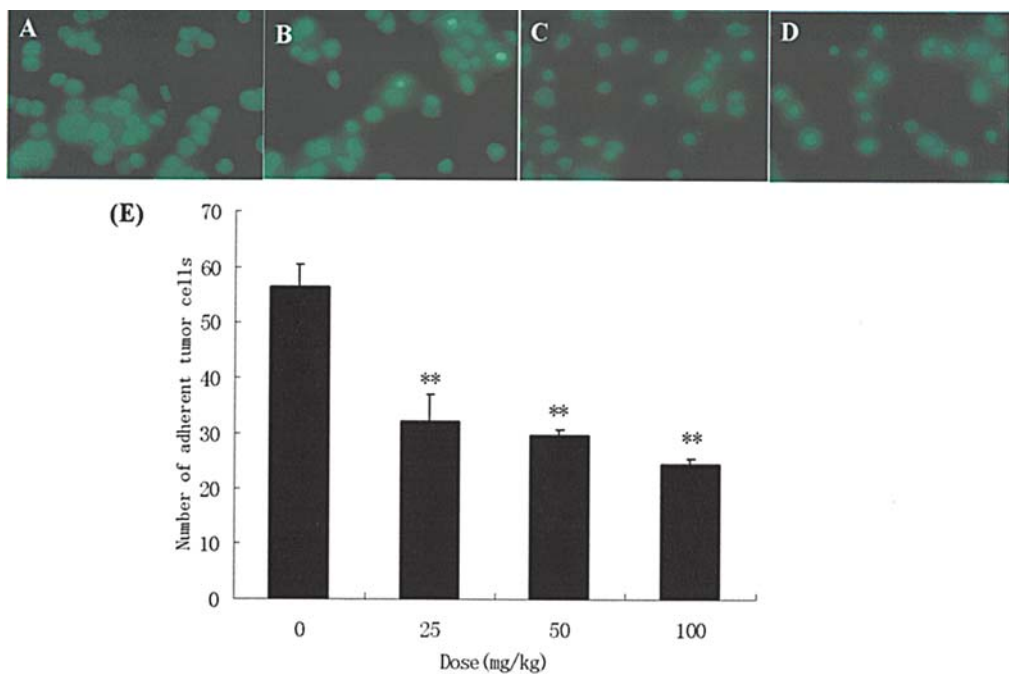


Figure 4. The inhibitory effect of *G/PS*-treated serum on the adhesion ability of PC-3M cells to HUVECs. The adhesion assay was performed with control serum and 25, 50, 100 mg/kg *G/PS*-treated serum. Adhesion ability of PC-3M cells to HUVECs was significantly inhibited by *G/PS*-treated serum. (A) Control; (B) 25 mg/kg *G/PS*-treated serum; (C) 50 mg/kg *G/PS*-treated serum; (D) 100 mg/kg *G/PS*-treated serum. Magnification x400. (E) Inhibition of PC-3M adhesion to HUVECs by *G/PS*-treated serum. n=5, mean ± SD. **P<0.01 vs control.

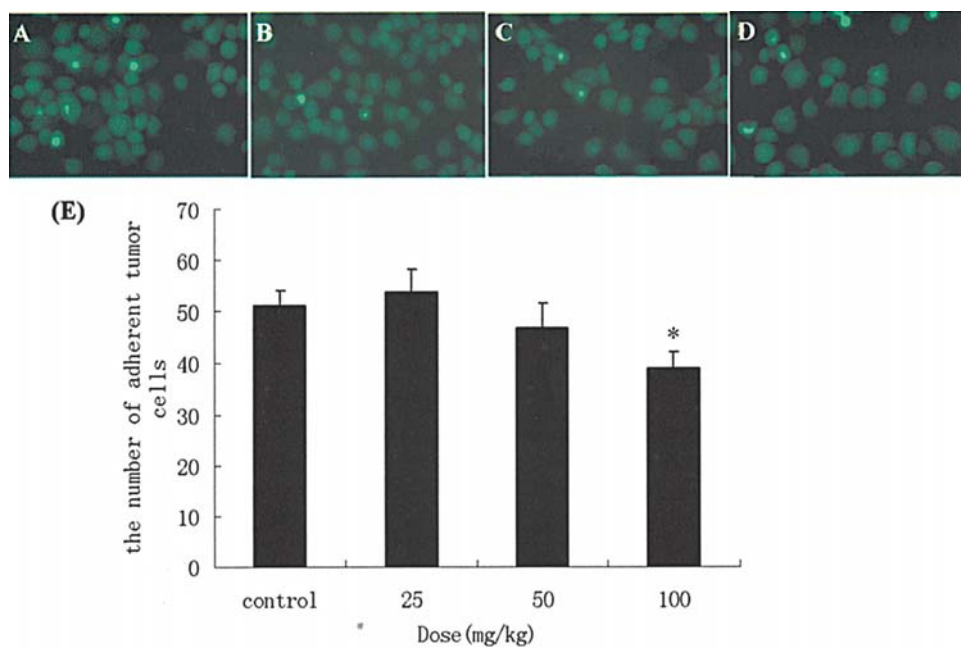


Figure 5. The effect of SAA-depleted *G/PS*-treated serum on the adhesion ability of PC-3M cells to HUVECs. SAA protein in *G/PS*-treated serum was depleted by immunodepletion assay using anti-SAA antibody. Then the adhesion assay was carried out using these SAA-depleted *G/PS*-treated sera. (A) SAA-depleted control; (B) 25 mg/kg SAA-depleted *G/PS*-treated serum; (C) 50 mg/kg SAA-depleted *G/PS*-treated serum; (D) 100 mg/kg SAA-depleted *G/PS*-treated serum. Magnification x400. (E) The inhibitory effect of *G/PS*-treated serum was partially abolished after the depletion of SAA. n=5, mean ± SD. *P<0.05 vs control.

differential expression patterns of these proteins would help us foster a better understanding of the pathophysiological molecular mechanisms of cancer (16). In addition, traditional medicines usually exert their effects through multitargets and multiapproaches, which might involve several protein

expression changes and modifications. Therefore, in our study, proteomic methods were applied in the *G/PS* study, hoping to elucidate the comprehensive serum protein expression after the drug treatment and to find the potential proteins related to anti-tumor mechanism of *G/PS*.

In this study, serum proteins were separated by their isoelectric points in the first IEF dimension, and then by their molecular mass using sodium dodecyl sulfate polyacrylamide gel electrophoresis (SDS-PAGE) in the second dimension. Comparing the proteins present in sera of control and *G/PS*-treated mice by computer-assisted comparative analysis, marked changes in protein profiles were discovered. Three protein spots showed relatively greater changes. These spots were in well separated areas and were excised from gels for MS analysis. The results revealed that these proteins were SAA, haptoglobin, which were up-regulated after the treatment of *G/PS*, and apolipoprotein A-II, which was down-regulated after the treatment.

Through function exploring, SAA was chosen for further study among the three proteins because of its important role in the process of cancer. SAA is one of the major acute-phase serum proteins, which appears at low concentration in health individuals but is increased up to 1000-fold in response to inflammation or various malignancies (17-19), suggesting its beneficial role in host defense. As the precursor of amyloid A (AA), SAA is probably involved in the progression of secondary amyloidosis and AA-amyloidosis (20). In addition, it is an apolipoprotein of high-density lipoprotein (HDL) and reported to participate in cholesterol metabolism and transport (21). More importantly, recent studies demonstrated that several functions for the SAA could be essential in neoplasia, which mainly attribute to the effect on the tumor cell adhesion and migration. These functions included inhibiting malignant cell attachment to extracellular matrix (22), inducing the expression of enzymes degrading the ECM (17,23,24), and stimulating leukocytes recruitment (7,25). In addition, it is regarded as the biomarker in several types of malignancies, such as gastric cancer (19), pancreatic cancer (26), non-small cell lung cancer (27) and nasopharyngeal cancer (28). According to these reports, we speculated that regulation of SAA expression might be one of the contributing factors to anti-tumor effects of *G/PS*.

Therefore, we used two different methods to test our hypothesis. Since adhesion of tumor cells to endothelial cells is a critical step in tumor metastasis, adhesion assay was chosen for the examination of the effect of SAA expression in the anti-tumor activity of *G/PS*. In the first approach, adhesion assay was performed with *G/PS*-treated serum and control serum. As shown in Fig. 4, the adhesion ability of PC-3M cells was significantly inhibited by *G/PS*-treated serum, in which the concentration of SAA is much higher than the control serum. In the second approach, we used SAA monoclonal antibody to immunodeplete the SAA protein in *G/PS*-treated sera and control serum, and then compared the adhesion abilities of tumor cells with immunodepleted sera, in all of which the SAA is absent. As shown in Fig. 5, the inhibition effect partially recovered after immunodepletion. Together, these results confirmed that up-regulation of SAA is one possible mechanism for *G/PS* to inhibit the tumor cell adhesion to endothelial cells, i.e., one possible anti-tumor mechanism of *G/PS*.

The mechanisms by which SAA protein inhibits the adhesion ability of tumor cells to endothelial cells remain unclear. One possible explanation may be related to the functional adhesion motifs of SAA. According to previous

reports, some proteins containing the peptide Tyr-Ile-Gly-Ser-Arg (YIGSR) and/or Arg-Gly-Asp (RGD) demonstrated inhibition activities in tumor cell invasion and metastasis, such as the multimeric YIGSR-containing peptide (Ac-Y16), and RGD-containing peptide (rhodostomin) (29-31). Both functional YIGSR-like and RGD-like motifs also present in the SAA protein (22). Therefore, it is plausible that both of the functional peptides for SAA were related to inhibit the adhesion of tumor cells to endothelial cells.

In addition, the dose of 100 mg/kg *G/PS* after removal of SAA still showed inhibition action of PC-3M cells adhesion to HUVECs, it suggested that other mechanisms might also be involved in this progression. Haptoglobin and apolipoprotein A-II, the other obviously changed proteins after the drug treatment, might be also related to the mechanism of the inhibition of *G/PS* on tumor growth. Further study on them is in progress in our laboratory.

In conclusion, this was the first investigation of the anti-tumor mechanism of *G/PS* by proteomic methods and some interesting results were obtained. We separated and identified three potential proteins, haptoglobin, apolipoprotein A-II and SAA from the serum sample of *G/PS*-treated mice by 2D gel electrophoresis combined with MS analysis. It was demonstrated that the SAA protein concentration in serum was correlated with inhibition of the adhesion ability of PC-3M cells to HUVECs. These results will be helpful in elucidating the anticancer mechanisms of *Ganoderma lucidum* polysaccharides.

Acknowledgements

This study was supported by the National Natural Science Foundation of China (No. 30171090, 30270528, 30572202, 30772571), 973 Program of the Ministry of Science and Technology in China (No. 2004CB518902), a research fund from The Ministry of Education of China (111 Project, No. B0700 and 985 Project).

References

1. Li YQ and Wang SF: Anti-hepatitis B activities of ganoderic acid from *Ganoderma lucidum*. *Biotechnol Lett* 28: 837-841, 2006.
2. Futrakul N, Panichakul T, Butthep P, Futrakul P, Jetanalin P, Patumraj P and Siriviriyakul P: *Ganoderma lucidum* suppresses endothelial cell cytotoxicity and proteinuria in persistent proteinuric focal segmental glomerulosclerosis (FSGS) nephrosis. *Clin Hemorheol Microcirc* 31: 267-272, 2004.
3. Tang W, Gao Y, Chen G, Gao H, Dai X, Ye J, Chan E, Huang M and Zhou S: A randomized, double-blind and placebo-controlled study of a *Ganoderma lucidum* polysaccharide extract in neurasthenia. *J Med Food* 8: 53-58, 2005.
4. Zhang HN, He JH, Yuan H and Lin ZB: *In vitro* and *in vivo* protective effect of *Ganoderma lucidum* polysaccharide on alloxan-induced pancreatic islets damage. *Life Sci* 73: 2307-2319, 2003.
5. Woo CW, Man RY, Siow YL, Choy PC, Wan EW, Lau CS and O K: *Ganoderma lucidum* inhibits inducible nitric oxide synthase expression in macrophages. *Mol Cell Biochem* 276: 165-171, 2005.
6. Sasaki T, Arai Y, Ikekawa T, Chihara G and Fukuoka F: Antitumor polysaccharides from some polyporaceae, *Ganoderma applanatum* (Pers.) Pat and *Phellinus linteus* (Berk. et Curt.) Aoshima. *Chem Pharm Bull* 19: 821-826, 1971.
7. Badolato R, Wang JM, Murphy WJ, Lloyd AR, Michiel DF, Bausserman LL, Kelvin DJ and Oppenheim JJ: Oppenheim, serum amyloid A is a chemoattractant: induction of migration, adhesion, and tissue infiltration of monocytes and polymorphonuclear leukocytes. *J Exp Med* 180: 203-209, 1994.

8. Cao QZ and Lin ZB: Antitumor and anti-angiogenic activity of *Ganoderma lucidum* polysaccharides peptide. *Acta Pharmacol Sin* 25: 833-838, 2004.
9. Sliva D, Labarrere C, Slivova V, Sedlak M, Lloyd FP Jr and Ho NW: *Ganoderma lucidum* suppresses motility of highly invasive breast and prostate cancer cells. *Biochem Biophys Res Commun* 298: 603-612, 2002.
10. Müller CI, Kumagai T, O'Kelly J, Seeram NP, Heber D and Koeffler HP: *Ganoderma lucidum* causes apoptosis in leukemia, lymphoma and multiple myeloma cells. *Leuk Res* 30: 841-848, 2006.
11. Kim HS, Kacew S and Lee BM: *In vitro* chemopreventive effects of plant polysaccharides (*Aloe barbadensis* miller, *Lentinus edodes*, *Ganoderma lucidum* and *Coriolus versicolor*). *Carcinogenesis* 20: 1637-1640, 1999.
12. Cheung WM, Hui WS, Chu PW, Chiu SW and Ip NY: *Ganoderma* extract activates MAP kinases and induces the neuronal differentiation of rat pheochromocytoma PC12 cells. *FEBS Lett* 486: 291-296, 2000.
13. Pan Y, Song QL, Lin YH, Lu N, Yu HM and Li XJ: GLB prevents tumor metastasis of Lewis lung carcinoma by inhibiting tumor adhesion actions. *Acta Pharmacol Sin* 26: 881-886, 2005.
14. Urieli-Shoval S, Linke RP and Matzner Y: Expression and function of serum amyloid A, a major acute-phase protein, in normal and disease states. *Curr Opin Hematol* 7: 64-69, 2000.
15. Christofori G: New signals from the invasive front. *Nature* 441: 444-450, 2006.
16. Li SQ, Qi HW, Wu CG, Zhang XJ, Yang SG, Zhao X, Wu Z, Wang Y, Que HP and Liu SJ: Comparative proteomic study of acute pulmonary embolism in a rat model. *Proteomics* 7: 2287-2299, 2007.
17. Gutfeld O, Prus D, Ackerman Z, Dishon S, Linke RP, Levin M and Urieli-Shoval S: Expression of serum amyloid A, in normal, dysplastic and neoplastic human colonic mucosa: implication for a role in colonic tumorigenesis. *J Histochem Cytochem* 54: 63-73, 2006.
18. Combaret V, Bergeron C, Bréjon S, Iacono I, Perol D, Négrier S and Puisieux A: Protein chip array profiling analysis of sera from neuroblastoma patients. *Cancer Lett* 228: 91-96, 2005.
19. Chan DC, Chen CJ, Chu HC, Chang WK, Yu JC, Chen YJ, Wen LL, Huang SC, Ku CH, Liu YC and Chen JH: Evaluation of serum amyloid A as a biomarker for gastric cancer. *Ann Surg Oncol* 14: 84-93, 2007.
20. Niemi K, Baumann MH, Kovanen PT and Eklund KK: Serum amyloid A (SAA) activates human mast cells which leads into degradation of SAA and generation of an amyloidogenic SAA fragment. *Biochim Biophys Acta* 1762: 424-430, 2006.
21. Van der Westhuyzen DR, Cai L, De Beer MC and De Beer FC: Serum amyloid A promotes cholesterol efflux mediated by scavenger receptor B-I. *J Biol Chem* 280: 35890-35895, 2005.
22. Preciado-Patt L, Levartowsky D, Prass M, Hershkovich R, Lider O and Fridkin M: Inhibition of cell adhesion to glycoproteins of the extracellular matrix by peptides corresponding to serum amyloid A. Toward understanding the physiological role of an enigmatic protein. *Eur J Biochem* 223: 35-42, 1994.
23. Brinckerhoff CE, Mitchell TI, Karmilowicz MJ, Kluge-Beckerman B and Benson MD: Autocrine induction of collagenase by serum amyloid A-like and beta 2-microglobulin-like proteins. *Science* 243: 655-657, 1989.
24. Migita K, Kawabe Y, Tominaga M, Origuchi T, Aoyagi T and Eguchi K: Serum amyloid A protein induces production of matrix metalloproteinases by human synovial fibroblasts. *Lab Invest* 78: 535-539, 1998.
25. Mullan RH, Bresnihan B, Golden-Mason L, Markham T, O'Hara R, FitzGerald O, Veale DJ and Fearon U: Acute-phase serum amyloid A stimulation of angiogenesis, leukocyte recruitment and matrix degradation in rheumatoid arthritis through an NF-kappaB-dependent signal transduction pathway. *Arthritis Rheum* 54: 105-114, 2006.
26. Yokoi K, Shih LC, Kobayashi R, Koomen J, Hawke D, Li D, Hamilton SR, Abbruzzese JL, Coombes KR and Fidler IJ: Serum amyloid A as a tumor marker in sera of nude mice with orthotopic human pancreatic cancer and in plasma of patients with pancreatic cancer. *Int J Oncol* 27: 1361-1369, 2005.
27. Khan N, Cromer CJ, Campa M and Patz EF Jr: Clinical utility of serum amyloid A and macrophage migration inhibitory factor as serum biomarkers for the detection of non-small cell lung carcinoma. *Cancer* 101: 379-384, 2004.
28. Cho WC, Yip TT, Yip C, Yip V, Thulasiraman V, Ngan RK, Yip TT, Lau WH, Au JS, Law SC, Cheng WW, Ma VW and Lim CK: Identification of serum amyloid a protein as a potentially useful biomarker to monitor relapse of nasopharyngeal cancer by serum proteomic profiling. *Clin Cancer Res* 10: 43-52, 2004.
29. Iwamoto Y, Nomizu M, Yamada Y, Ito Y, Tanaka K and Sugioka Y: Inhibition of angiogenesis, tumour growth and experimental metastasis of human fibrosarcoma cells HT1080 by a multimeric form of the laminin sequence Tyr-Ile-Gly-Ser-Arg (YIGSR). *Br J Cancer* 73: 589-595, 1996.
30. Nicosia RF and Bonanno E: Inhibition of angiogenesis *in vitro* by Arg-Gly-Asp-containing synthetic peptide. *Am J Pathol* 138: 829-833, 1991.
31. Chiang HS, Yang RS and Huang TF: The Arg-Gly-Asp-containing peptide, rhodostomin, inhibits *in vitro* cell adhesion to extracellular matrices and platelet aggregation caused by saos-2 human osteosarcoma cells. *Br J Cancer* 71: 265-270, 1995.